$$W^{(1/2,\,0)} = W_{\mathrm{cl}}\,\varphi^{(1/2,\,0)}(\zeta); \tag{3}$$

$$\varphi^{(1/2)}(\zeta) = \frac{3\sqrt{3}}{8}\pi\left\{\frac{\partial}{\partial\zeta}\frac{\Phi_{1/3}\left(\frac{i}{\zeta}\right)}{\zeta^2} - \frac{\zeta^2}{3}\frac{\partial^3}{\partial\zeta^3}\frac{\Phi_{1/3}\left(\frac{i}{\zeta}\right)}{\zeta} - \frac{\sqrt{3}}{2\pi}\frac{1}{\zeta^2}\right\}, \tag{3a}$$

$$\varphi^{(0)}(\zeta) = \frac{3\sqrt{3}}{8}\pi\left\{\frac{\partial}{\partial\zeta}\frac{\Phi_{1/3}\left(\frac{i}{\zeta}\right)}{\zeta^2} - \frac{\sqrt{3}}{2\pi}\frac{1}{\zeta^2}\right\};$$

$$\Phi_\nu(z) = i^{-\nu}[J_\nu(z) - \mathbf{J}_\nu(z)] + i^{\nu}[J_{-\nu}(z) - \mathbf{J}_{-\nu}(z)], \tag{3b}$$

where J_ν is the Bessel function and $\mathbf{J}_\nu$ the Anger's function.

For relatively small energies ($\zeta \ll 1$) of the radiating particles, we obtain from the above formulas:

$$\frac{W^{(1/2)}}{W^{(0)}} \approx 1 + \frac{8}{3}\zeta^2 - \frac{275\sqrt{3}}{18}\zeta^3 + \ldots,$$

which shows that the spin is involved only in quantities ζ^2, i.e., in quantities of second order in h. This is why Schwinger's spinless calculation[4], correct to the first order in h, gives the same result as the first quantum correction for particles with spin made by Sokolov, Klepikov and Ternov[7]. Nelipa's evaluation cannot be correct because it does not depend on h.

For extreme relativistic energies ($\zeta \gg 1$) the radiation of a spinless particle differs essentially from that of an electron. This may be seen on the graph, where the spectra of the electron (solid line) and of a spinless particle (dashes-crosses) have been plotted. For comparison under the same circumstances, the spectrum given by classical theory has also been plotted (dotted line). The limit of the spectrum in the high frequency region is given by the energy-momentum conservation law ($\omega_{\max} \approx E/h$).

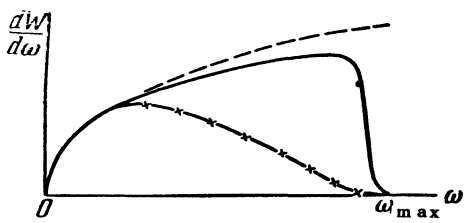

The particularities of the spectra are obvious and do not need further explanations. As it was noted by Sokolov, the main difference between radiation spectra of an electron and a spinless particle is related to the appearance of the electronic magnetic moment which takes place for high energies ($\zeta \gg 1$). This question will be considered in more detail elsewhere.

[1] N. F. Nelipa, J. Exper. Theoret. Phys. USSR **27**, 427 (1954)

[2] A. N. Matveev, Thesis, Moscow State University, 1954

[3] D. Ivanenko and A. Sokolov, Dokl. Akad. Nauk SSSR **59**, 1551 (1948)

[4] J. Schwinger, Phys. Rev. **75**, 1912 (1949)

[5] A. A. Sokolov and I. M. Ternov, J. Exper. Theoret. Phys. USSR **25**, 698 (1953)

[6] J. Schwinger, Proc. Nat. Acad. Sci. **40**, 132 (1954)

[7] A. A. Sokolov, N. P. Klepikov and I. M. Ternov, J. Exper. Theoret. Phys. USSR **24**, 249 (1953)

Translated by E. S. Troubetzkoy
258

Investigation of the Structure of Extensive Air Showers at Sea Level

A. T. Abrosimov, A. A. Bedniakov, V. I. Zatsepin, Iu. A. Nechin, V. I. Solov'eva, G. B. Khristiansen and P. S. Chikin

(Submitted to JETP editor May 3, 1955)
J. Exper. Theoret. Phys. USSR 29, 693-696 (November, 1955)

In reference 1 a qualitative indication was found that the spatial distribution of the electron component of extensive air showers at sea level is essentially different from that expected from the point of view of the electron-photon picture of the development of showers in the atmosphere. In the summer of 1953 we carried out in Moscow a detailed investigation of the spatial distribution of different components of extensive air showers at small distances from the axis of the shower by the method of correlated hodoscopes*. We report below preliminary results.

To study the spatial distribution of electrons of the shower, density indicators were used, consisting of groups of 24 counters of identical areas, each of which was contained in a hodoscopic cell of a neon hodoscope[2]. In the apparatus were used counters of three different areas: 24, 100 and 330 cm^2, which made it possible to study the

showers in a wide range of particle densities. Forty-seven density indicators were distributed uniformly in a circle of radius 7 m, and 9 indicators were at distances 15, 20 and 30 m from the center of the arrangement (Fig. 1). All density indicators were placed under a thin veneer roof (2.5 gm/cm^2).

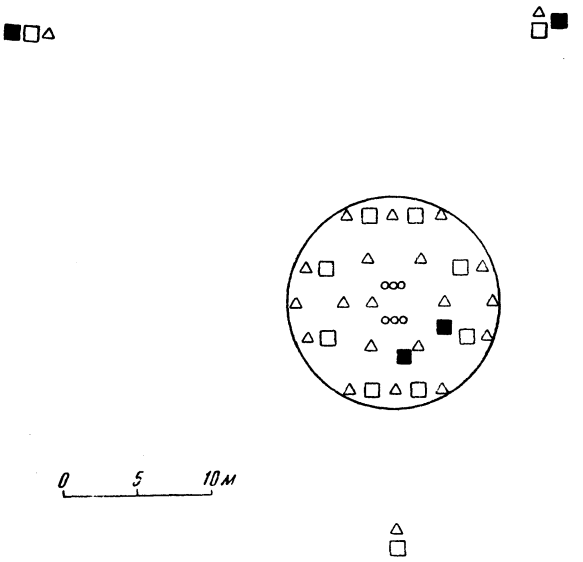

FIG. 1. Arrangement of apparatus. Key: □ - 24 counters of area 330 cm^2 each, △ - 24 counters of area 100 cm^2 and 24 counters of area 24 cm^2 each, ■ - detector of penetrating particles, O - group of counters 4 × 330 cm^2, inserted in coincidence. Six of such groups constitute an independent indicator of density.

For the study of nuclearly interacting particles, detectors of penetrating particles were used. These consisted of three trays of counters, shielded from all sides by lead and iron (Fig. 2). In the arrangement there were four such detectors, placed at various intervals from the center of the apparatus (Fig. 1). The apparatus was triggered by the coincidence of six groups of counters, placed in the center of the apparatus (Fig. 1) and belonging at the same time to one of the density indicators. The area of a single group of counters was 4 × 330 cm^2.

When the axis of the shower fell in the central part of the apparatus, the totality of data of all density indicators gave the distribution of flux density of shower particles near the axis of the shower. In this case, assuming that the showers have axial symmetry, it was possible to define the position of the axis of the shower. The position of the axis was defined to an accuracy of 1 m; this accuracy was determined by the basic intervals between density indicators (~ 3 m), the sharpness of increase of density of current of particles towards the axis of the shower, and the accuracy with which each indicator registered the density of shower particles (~ 30%).

For each shower with axis in the central part of the apparatus, it was possible to construct the function of spatial distribution. The density indicators gave the magnitude of the flux density of shower particles at different distances r from the axis of the shower. The density of particles ρ at the position of an indicator was defined by the formula

$$\rho\sigma = \ln \frac{n}{n-m}, \qquad (1)$$

where n is the total number of counters in the indicator, m is the number of discharged counters, σ is the area of each counter.

Insofar as the accuracy of definition of the

curve of spatial distribution of individual showers is low, we carried out an averaging with respect to the number of particles of curves of spatial distribution for showers lying in a sufficiently narrow interval. We defined the total number of particles in the shower N using the spatial distribution experimentally obtained at distances of 2 to 20 m and beyond this, making a smooth transition to the distribution $1/r^{2.6}$ justified according to reference 3 for large distances, beginning at 70 m from the axis of the shower.

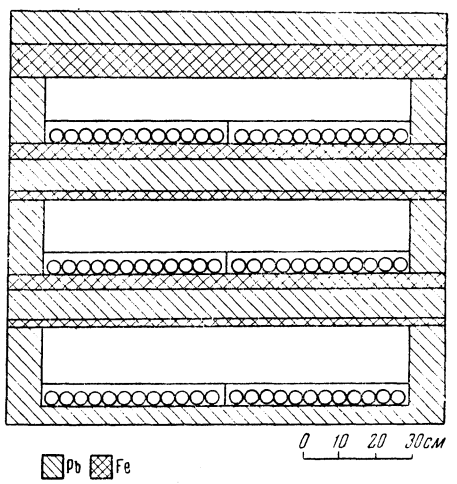

FIG. 2. Section of the detector of penetrating particles. The shielding of the particles from the ends is the same as from the sides.

Because of the inclusion of all counters of the detector in the hodoscope it was possible to distinguish whether the particle incident on the detector was nuclearly interacting. In order to do this, we used the property of a nuclearly interacting particle, i.e., it has a high probability of creating an electron-nuclear shower in going through dense material. The presence of electron-nuclear showers was observed by the coincidence of a large number (≥ 3) of counters in the second and third rows of the detector. The data obtained in this way were analyzed statistically. The mean density of the flux of nuclearly interacting particles $\rho_{(n.i.)}$ was defined by the formula

$$\rho_{n.i.} \sum = \frac{\ln [k/(k-l)]}{1-\exp(-\mu d)}, \qquad (2)$$

where k is the number of showers with a number of particles in the interval N, $N + \Delta N$ and with axes in the interval r, $r + \Delta r$ from the center of the detector, in which case in l out of k showers, the detector of area Σ registers the presence of nuclearly interacting particles; $1/\mu$ g/cm^2 is the interaction length of nuclearly interacting particles, calculated on the assumption that the effective cross section for production of electron-nuclear showers is geometrical; d g/cm^2 is the thickness of material in which the nuclearly interacting particle gives rise to electron-nuclear showers.

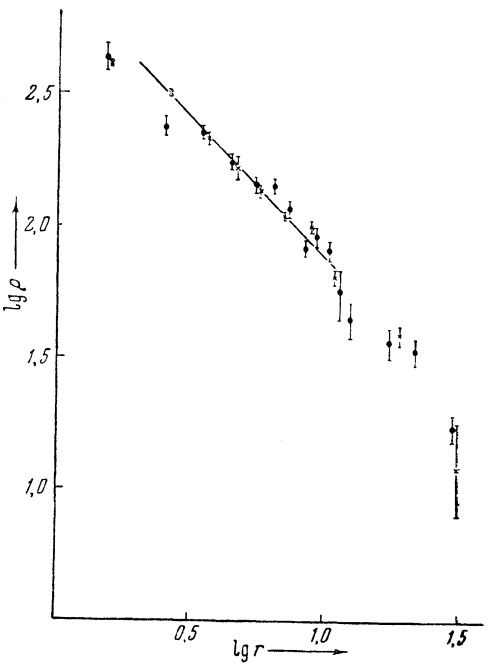

FIG. 3. Spatial distribution of charged particles in extensive air showers with number of particles: ×-$\overline{N} = 4 \times 10^4$, ●-$\overline{N} = 4 \times 10^5$. Solid curve-spatial distribution obtained in a mountainous region (Pamir[4]), (at 3860 m above sea level).

In Fig. 3 are given the spatial distributions of densities of electron current from two groups of showers, differing from each other in number of particles N by an average factor of 10. The spatial distribution for one group of showers was obtained by averaging over 50 showers with numbers of particles lying in the interval $2 \times 10^5 - 10 \times 10^5$ ($\overline{N} = 4 \times 10^5$); the spatial distribution for the other group of showers was obtained by averaging over 50 showers with particle numbers in the interval $2 \times 10^4 - 6 \times 10^4$ ($\overline{N} = 4 \times 10^4$). At distances from 2 to 10 m the spatial distribution** obtained can be approximated by the function $1/r^n$, where $n = 0.93 \pm 0.08$ for showers with $\overline{N} = 4 \times 10^5$ and $n = 1.0 \pm 0.05$ for showers with $\overline{N} = 4 \times 10^4$.

The spatial distribution of nuclearly interacting particles is given in Fig. 4. The data refer to

showers with numbers of particles in the interval $1.5 \times 10^4 - 4 \times 10^5$ ($\overline{N} = 8 \times 10^4$). The curve goes as $1/r^n$, where $n = 1.1 \pm 0.2$.

A very important conclusion from the results obtained is the presence in showers observed at sea level of a sharply defined core. In fact, right up to the axis of the shower, at least to 2 m, in showers of various energies, a sharp rise was observed in the density of the electron and nuclearly interacting component, varying approximately as $1/r$. We note that the spatial distribution $1/r$ along the axis is characteristic of the electron-photon cascade showers near the maximum of their development. It is essential that the sharpness of the core of the shower depends not only on the total energy of the shower, but also on the stage of development in the atmosphere. This conclusion follows from comparison of our data with corresponding data of references 4 and 5, relating to a mountainous region. The comparison is made on Figs. 3 and 4, where account is taken of the difference in density of air at sea level and in the mountainous region. The experimental data obtained indicate the identity of structure of the central region of extensive showers at two different stages of their development.

Consequently, a process should exist which leads to a continual renovation of this region of the shower. In the lower layers of the atmosphere this process is the continual transfer of energy from nuclearly interacting particles of high energy, concentrated in the core of the shower, to the flux of electrons and nuclearly interacting particles, studied by us, of the central part. We note that the spatial distribution is $1/r$.

In conclusion, the authors express their deep appreciation to G. T. Zatsepin for valuable advice and discussion of results and to N. A. Dobrotin for a great deal of help and a constant interest in this work.

The authors express also their thanks to G. V. Bogoslovskii, B. V. Subbotin and M. S. Tuliankina, who took part in the carrying out of measurements.

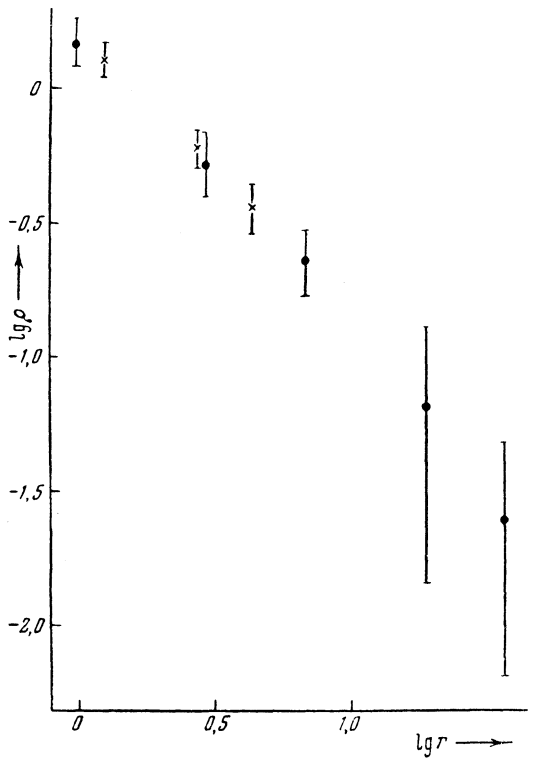

FIG. 4. Spatial distribution of nuclearly interacting particles: ●-results of the present work, ×-results obtained in a mountainous region (Pamir[5]), (at 3860 m above sea level).

* The method of correlated hodoscopes is based on the measurement of the density of the shower by a hodoscopic system of counters simultaneously at several places of the plane on which the shower impinges.

** A detailed analysis shows that the inaccuracy in the definition of the position of the axis distorts the form of the spatial distribution function at distances less than 2 m from the axis.

[1] L. Kh. Eidus, Dokl. Akad. Nauk SSSR **81**, 1035 (1951)

[2] L. N. Korablev, Dokl. Akad. Nauk SSSR **62**, 215 (1948)

[3] L. Kh. Eidus, N. M. Blinova et al, Dokl. Akad. Nauk SSSR **80**, 577 (1951)

[4] Iu. N. Vavilov, S. I. Nikol'skii and E. I. Tukish, Dokl. Akad. Nauk SSSR **93**, 233 (1953)

[5] Iu. N. Vavilov, S. I. Nikol'skii and V. P. Sarantsev, J. Exper. Theoret. Phys. USSR **28**, 505 (1955); Soviet Phys. **1**, 399 (1955)

Translated by G. E. Brown
255